



THE UNIVERSITY *of* EDINBURGH

Edinburgh Research Explorer

## Dimethyl fumarate improves white matter function following severe hypoperfusion

### Citation for published version:

Fowler, JH, McQueen, J, Holland, P, Manso Sanz, Y, Marangoni, M, Scott, F, Chisholm, E, Scannevin, RH, Hardingham, GE & Horsburgh, K 2018, 'Dimethyl fumarate improves white matter function following severe hypoperfusion: involvement of microglia/macrophages and inflammatory mediators', *Journal of Cerebral Blood Flow and Metabolism*, vol. 38, no. 8, pp. 1354-1370. <https://doi.org/10.1177/0271678X17713105>

### Digital Object Identifier (DOI):

[10.1177/0271678X17713105](https://doi.org/10.1177/0271678X17713105)

### Link:

[Link to publication record in Edinburgh Research Explorer](#)

### Document Version:

Publisher's PDF, also known as Version of record

### Published In:

Journal of Cerebral Blood Flow and Metabolism

### General rights

Copyright for the publications made accessible via the Edinburgh Research Explorer is retained by the author(s) and / or other copyright owners and it is a condition of accessing these publications that users recognise and abide by the legal requirements associated with these rights.

### Take down policy

The University of Edinburgh has made every reasonable effort to ensure that Edinburgh Research Explorer content complies with UK legislation. If you believe that the public display of this file breaches copyright please contact [openaccess@ed.ac.uk](mailto:openaccess@ed.ac.uk) providing details, and we will remove access to the work immediately and investigate your claim.



# Dimethyl fumarate improves white matter function following severe hypoperfusion: Involvement of microglia/macrophages and inflammatory mediators

Jill H Fowler<sup>1</sup>, Jamie McQueen<sup>1,2</sup>, Philip R Holland<sup>1,3</sup>, Yasmina Manso<sup>1,4</sup>, Martina Marangoni<sup>1,5</sup>, Fiona Scott<sup>1</sup>, Emma Chisholm<sup>1</sup>, Robert H Scannevin<sup>6</sup>, Giles E Hardingham<sup>2,7</sup> and Karen Horsburgh<sup>1,8</sup>

## Abstract

The brain's white matter is highly vulnerable to reductions in cerebral blood flow via mechanisms that may involve elevated microgliosis and pro-inflammatory pathways. In the present study, the effects of severe cerebral hypoperfusion were investigated on white matter function and inflammation. Male C57Bl/6J mice underwent bilateral common carotid artery stenosis and white matter function was assessed at seven days with electrophysiology in response to evoked compound action potentials (CAPs) in the corpus callosum. The peak latency of CAPs and axonal refractoriness was increased following hypoperfusion, indicating a marked functional impairment in white matter, which was paralleled by axonal and myelin pathology and increased density and numbers of microglia/macrophages. The functional impairment in peak latency was significantly correlated with increased microglia/macrophages. Dimethyl fumarate (DMF; 100 mg/kg), a drug with anti-inflammatory properties, was found to reduce peak latency but not axonal refractoriness. DMF had no effect on hypoperfusion-induced axonal and myelin pathology. The density of microglia/macrophages was significantly increased in vehicle-treated hypoperfused mice, whereas DMF-treated hypoperfused mice had similar levels to that of sham-treated mice. The study suggests that increased microglia/macrophages following cerebral hypoperfusion contributes to the functional impairment in white matter that may be amenable to modulation by DMF.

## Keywords

Electrophysiology, cerebrovascular disease, inflammation, microglia, white matter

Received 22 December 2016; Revised 30 March 2017; Accepted 25 April 2017

## Introduction

The integrity and connectivity of the brain's white matter are critical in regulating efficient neuronal communication and maintaining cognitive function. The

<sup>5</sup>Current Address: Department of Health Sciences, University of Florence, Florence, Italy

<sup>6</sup>Biogen, Cambridge, Massachusetts, USA

<sup>7</sup>The UK Dementia Research Institute at The University of Edinburgh

<sup>8</sup>Centre for Cognitive Ageing and Cognitive Epidemiology, University of Edinburgh, Edinburgh, UK

### Corresponding authors:

Jill H Fowler, Centre for Neuroregeneration, University of Edinburgh, Chancellor's Building, 49 Little France Crescent, Edinburgh EH16 4SB, UK.

Email: Jill.Fowler@ed.ac.uk

Karen Horsburgh, Centre for Neuroregeneration, University of Edinburgh, Chancellor's Building, 49 Little France Crescent, Edinburgh EH16 4SB, UK.

Email: Karen.Horsburgh@ed.ac.uk

<sup>1</sup>Centre for Neuroregeneration, University of Edinburgh, Edinburgh, UK

<sup>2</sup>Centre for Integrative Physiology, University of Edinburgh, Edinburgh, UK

<sup>3</sup>Current Address: Department of Basic and Clinical Neuroscience, Institute of Psychiatry, Psychology and Neuroscience, King's College London, London, UK

<sup>4</sup>Current Address: Developmental Neurobiology and Regeneration Lab, Parc Científic de Barcelona, Spain

key functional cellular elements of white matter tracts are myelinated axons, the integrity of which is dependent on a constant supply of energy to enable accuracy and speed of action potential conduction between different brain regions.<sup>1</sup> Myelinated axons and oligodendrocytes in white matter are highly vulnerable to reductions in cerebral blood flow.<sup>2–4</sup> White matter hyperintensities, frequently detected in MRI scans from the brains of elderly individuals and those with dementia, are closely linked to cerebral hypoperfusion.<sup>5,6</sup> A causal relationship has been shown in mouse models, whereby chronic hypoperfusion leads to white matter injury as detected using DT-MRI<sup>7</sup> and pathological investigations which show impaired axon-glial integrity and robust microgliosis.<sup>8,9</sup>

At a functional level, the burden of white matter hyperintensity load has been correlated with cognitive deficits.<sup>10,11</sup> We have demonstrated that chronic hypoperfusion in mice initially induces a selective deficit in spatial working memory<sup>8</sup> that progresses to encompass deficits in spatial reference memory in the longer term.<sup>12</sup> Oxygen-glucose deprivation in *ex vivo* brain slices induces an irreversible conduction failure of evoked compound action potential (CAP) assessed with electrophysiology in the corpus callosum, which is accompanied by axonal pathology and oligodendrocyte death.<sup>13</sup>

At a mechanistic level, an elevated inflammatory response is implicated in the pathogenesis of white matter pathology following cerebral hypoperfusion. We have reported increased numbers of microglia in white matter following mild chronic hypoperfusion<sup>8,12,14</sup> which is also observed in more severe models.<sup>15</sup> In white matter, increased levels of cytokines and chemokines such as TNF $\alpha$ , IL-1 $\beta$ , IL-6 and MCP1<sup>16,17</sup> and increased levels of oxidised proteins and DNA are present following chronic hypoperfusion,<sup>18–20</sup> which are both implicated in microglial-mediated damage.<sup>9,21</sup> Pharmacological compounds that reduce activated microglia and pro-inflammatory pathways have beneficial effects on white matter after chronic hypoperfusion<sup>22–24</sup> and confer protective effects against cognitive deficits.<sup>25</sup> Similarly, drugs which reduce pro-inflammatory microglia in white matter can improve CAP amplitude after traumatic brain injury (TBI) and experimental autoimmune encephalitis (EAE; a mouse model of multiple sclerosis).<sup>26,27</sup>

Dimethyl fumarate (DMF), an anti-inflammatory drug,<sup>28</sup> has neuroprotective effects in a number of mouse models of neurodegenerative diseases<sup>29</sup> which are paralleled by a reduction in microgliosis.<sup>30–32</sup> Similarly, DMF has neuroprotective effects in intracerebral or subarachnoid haemorrhage and focal cerebral ischaemia<sup>33–36</sup> where it can improve neurological deficits and reduce microglial activation.<sup>35,36</sup> DMF or monomethyl fumarate (MMF; the active metabolite

of DMF) treatment of microglial cultures can inhibit lipopolysaccharide-induced production of pro-inflammatory cytokines and switch the molecular phenotype of microglia to an alternatively activated, neuroprotective one.<sup>37–39</sup> Of relevance to white matter damage, DMF has been shown to reduce demyelination, axonal damage, and improve survival and disease course in EAE.<sup>40–42</sup>

The present study aimed to test the hypothesis that severe hypoperfusion would cause a functional and structural impairment of white matter and increased neuroinflammation and that DMF would improve white matter function following hypoperfusion by modulating neuroinflammation.

## Materials and methods

### Animals and surgery

Adult male C57Bl/6J mice (aged 3–4 months, group housed, obtained from Charles River UK, 12 h light/dark cycle, free access to food and water) underwent severe chronic cerebral hypoperfusion via bilateral common carotid artery stenosis using microcoils under isoflurane anaesthesia. A 0.18 mm internal diameter microcoil was applied to the left and a 0.16 mm microcoil was applied to the right common carotid artery as previously described.<sup>15</sup> Sham mice underwent identical surgical procedure except the microcoils were not placed on the arteries. To assess if hypoperfusion could induce functional deficit in the corpus callosum and to determine the pathological correlates, CAPs were assessed in a cohort of mice using electrophysiology (hypoperfusion  $n=12$ , sham  $n=12$ ). To determine the effects of DMF on white matter function and pathology, two experimental cohorts were studied. Cohort 1 underwent assessment of white matter pathology (sham vehicle  $n=7$ ; sham DMF  $n=8$ ; hypoperfused vehicle  $n=15$ ; hypoperfused DMF  $n=11$ ). Cohort 2 underwent electrophysiology and inflammatory-related multiplex analysis (sham vehicle  $n=10$ ; sham DMF  $n=10$ ; hypoperfused vehicle  $n=16$ ; hypoperfused DMF  $n=13$ ). Group size was determined using power calculations from electrophysiology data. Mice were closely monitored following surgery and those that had a poor recovery after surgery were culled. The initial and final cohort sizes are indicated in supplementary Table 1.

In all cohorts, mice were coded and randomly assigned to experimental groups. Mice were terminated seven days following surgery. The surgery was undertaken by an experimenter who was blinded to drug treatment group. The data analysis was conducted by researchers blinded to experimental grouping. All experiments were conducted under the UK Home

Office Animals (Scientific Procedures) Act 1986, in agreement with local ethical and veterinary approval (Biomedical Research Resources, University of Edinburgh) and the ARRIVE guidelines.

### *Laser speckle contrast imaging*

Details of laser speckle contrast imaging are presented in the supplemental material.

### *Administration of DMF*

DMF (Sigma, UK) was administered twice daily (8 a.m. and 5 p.m.) by oral gavage at 100 mg/kg body weight in 0.8% hydroxypropyl methylcellulose (Sigma, UK) vehicle as previously described.<sup>41</sup> Control animals received vehicle only. Administration of DMF or vehicle began 24 h prior to surgery and continued for seven days. Investigators administering DMF or vehicle were blinded as to surgical intervention.

### *Electrophysiology*

Mice were terminated by cervical dislocation followed by decapitation. Brains were rapidly dissected, placed in a cell strainer and submerged in ice-cold oxygenated artificial cerebrospinal fluid (aCSF) (189 mM sucrose; 10 mM D-glucose; 26 mM NaHCO<sub>3</sub>; 3 mM KCl; 5 mM MgCl<sub>2</sub>; 5; 0.1 mM CaCl<sub>2</sub>; 1.25 mM NaH<sub>2</sub>PO<sub>4</sub>) for 2–3 min. Brains were then affixed to a metal vibratome plate and placed in a bath of oxygenated ice-cold sucrose-aCSF. A single 400  $\mu$ m coronal slice approximately –1.2––1.7 mm from bregma was cut using a vibratome (Zeiss, Germany), and then transferred to a warmed incubation chamber (32–35°C) containing oxygenated aCSF (10 mM D-Glucose; 26 mM NaHCO<sub>3</sub>; 5 mM KCl; 2 mM CaCl<sub>2</sub>; 124 mM NaCl; 1.25 mM NaH<sub>2</sub>PO<sub>4</sub>; 1.3 mM MgSO<sub>4</sub>). The incubation chamber was then allowed to return to room temperature for at least 1 h prior to slice recording.

For recording, individual slices were transferred to the slice chamber, super-perfused with oxygenated room temperature aCSF (2–3 ml/min), secured with a slice anchor and allowed to rest for 30 min. Recording electrodes (1–5 M $\Omega$ ) were pulled from borosilicate glass capillaries and filled with aCSF, connected to the headstage via the Ag/AgCl wire and lowered into the corpus callosum. A bipolar stimulating electrode was connected to the stimulus isolation unit and lowered into the corpus callosum. Constant current square wave pulses were delivered at 0.2 Hz for eight sweeps and the average response of the final four sweeps used for analysis.<sup>43</sup> The data were digitised at 200 kHz, amplified at 100 $\times$  and low pass filtered at 5 kHz then recorded on Clampex 10.3.

CAPs were evoked, whilst holding the stimulus intensity constant (100  $\mu$ s duration, 0.2 Hz), and recorded at 0.5 mm increments from 1 to 2.5 mm by moving the recording electrode. The post-stimulus latency of the CAP peak was then measured as a functional index of conduction velocity. For statistical comparison between groups, the CAP was measured at a distance of 2.5 mm apart.

Axonal health can be assessed by assaying changes in axonal excitability or axonal 'refractoriness'.<sup>43,44</sup> To assess the axon refractoriness, a single control stimulus was given followed by a paired pulse of equal intensity separated by a variable time window decreasing from 10 to 1.5 ms in 0.5 ms increments. The control amplitude was subtracted from the paired pulse response to leave only the second pulse which was measured and normalised to the % of the baseline CAP. The results were graphed versus the inter-pulse interval, and the interval that results in a 50% reduction in CAP was used for statistical comparisons.

### *Tissue processing and immunohistochemistry*

To determine the effects of severe hypoperfusion on white matter function and pathology, one cohort underwent electrophysiology, and an adjacent 2 mm slice of tissue was processed for paraffin embedding, then 8  $\mu$ m sections were cut with a microtome. All other mice were deeply anesthetized with 5% isoflurane and transcardially perfused with 20 ml of 0.9% heparinized phosphate buffer saline (PBS) and then 20 ml of 4% paraformaldehyde (PFA) in 0.9% PBS seven days after surgery. After perfusion, brains were removed, postfixed in 4% PFA for 24 h and then transferred to 30% sucrose in PBS for 48 h. Brains were frozen in isopentane at –42°C for 2 min. Thirty micrometres coronal sections were cut using a cryostat (Leica) and stored in cryoprotective medium (30% glycerol/30% ethylene glycol in phosphate buffer) at –20°C until use. Cryostat sections were dehydrated through an increasing alcohol series, and then immersed in xylene for 10 min before being rehydrated through a decreasing alcohol series. Sections were then equilibrated in PBS for 5 min before antigen retrieval (if required). A 10 mM citric acid (pH 6) antigen retrieval was carried out for Iba1, MBP and MAG staining. Sections were blocked using 10% normal serum and 0.5% BSA for 1 h at room temperature. Primary antibodies were made up in blocking solution and sections were incubated in primary antibody at 4°C overnight. The following day, the sections were incubated with secondary antibody in PBS for 2 h at room temperature. Coverslips were mounted using Vectashield HardSet mounting medium with or without DAPI. The following primary antibodies were used in the study: antimyelin-associated

glycoprotein (MAG) (1:200, Abcam) as an index of axon-glia integrity; anti-myelin basic protein (MBP) to label myelin (1:100, Millipore); anti-ionised calcium-binding adaptor receptor molecule 1 (Iba1) to label microglia (1:100, Menarini); anti-amyloid precursor protein (APP) to label axonal damage (1:200, Millipore); antiadenomatous polyposis coli protein CC1 (APC) to label oligodendrocyte cell bodies (1:200, Calbiochem); antineuronal-glia antigen (NG2) to label oligodendrocyte progenitor cells (1:100, Millipore). Alexa Fluor 488 and 555 conjugated secondary antibodies (1:500) were purchased from Life Technologies Ltd (UK).

### *Image acquisition and analysis*

All images were acquired using a confocal microscope (Leica TCS SP5) with either a 20 $\times$  air or a 40 $\times$  oil-immersion objective, pinhole of 1 Airy unit and 1024  $\times$  1024 pixel resolution. MBP, MAG, APP, and Iba1 immunostainings were acquired as one single image, while CC1 and NG2 were acquired as a 5  $\mu$ m stack. Images were acquired at the corpus callosum from the right hemisphere above the lateral ventricle at the stereotactic co-ordinates, lateral 2.40  $\pm$  0.1 mm, Bregma  $-1.5 \pm 0.1$  mm. Quantitative measurements were performed using imageJ (FIJI) software. The number of Iba-1 positive cells was counted in three defined areas, and the average was used for statistical purposes. Mean fluorescence intensity (MBP, MAG immunostaining) or the percentage area of positive staining (Iba1 immunostaining) or number of cells/volume (CC1/NG2 immunostaining) were measured at the corpus callosum which was manually outlined using a free-hand tool. The number of swollen axons (axonal bulbs) in APP immunostained sections was counted in three defined areas along the corpus callosum and the average was used for statistical purposes. Observers were blind to surgery procedure and drug treatment.

### *Inflammatory-related protein multiplex*

Brain homogenates were assayed for inflammatory-related molecules using a Bio-plex mouse cytokine and chemokine assay (Biorad), which allows the detection of multiple inflammatory-related molecules in the same sample. A 1.8 mm section rostral to the brain slice used for electrophysiology was snap frozen in liquid nitrogen and stored at  $-80^{\circ}\text{C}$ . Tissue was weighed and homogenised in 5  $\times$  volume of tissue lysing solution (Bioplex cell lysis kit, made according to manufacturer's instructions), and then sonicated for 5 s at 10% amplitude. Samples were spun at 5000  $g$  at  $4^{\circ}\text{C}$ , and then the supernatant was collected and stored at  $-80^{\circ}\text{C}$ . Total protein concentration was determined

using a Thermo Scientific Pierce BCA Protein Assay Kit and samples were diluted with bioplex cell lysis buffer to obtain a final total protein concentration of 13 mg/ml. Samples were then diluted to 8 mg/ml in bioplex sample buffer diluent before they underwent the multiplex assay according to the manufacturer's instructions. The levels of seven inflammatory-related molecules were measured: interleukin-6 (IL-6), interleukin-1 $\beta$  (IL-1 $\beta$ ), interferon- $\gamma$  (IFN- $\gamma$ ), keratinocyte chemoattractant (KC), monocyte chemoattractant-1 (MCP-1), macrophage inflammatory protein 1- $\alpha$  (MIP-1 $\alpha$ ) and vascular endothelial growth factor (VEGF) in duplicate with standards (sham vehicle  $n=8$ ; sham DMF  $n=8$ , hypoperfused vehicle  $n=11$ ; hypoperfused DMF  $n=11$ ). One animal from each of the hypoperfusion groups and two animals from each of the sham groups were randomly selected for omission from this experiment due to the space restrictions of the 96-well plate. Standards included in each kit were used to generate standard curves for each analyte, and then the mean fluorescence intensity for each analyte was calculated with five-point logistic regression using Bio-plex workstation software (Biorad).

### *Statistics*

Analysis and graphs were generated using Prism GraphPad 5.0 software. Data from the electrophysiology and related pathology cohorts were normally distributed and analysed using Student's  $t$  test for independent samples. Associations between electrophysiology data and microglia numbers were analysed with Pearson's correlation analysis. Other data, in which the effect of surgery and drug treatment or cerebral blood flow were investigated, were analysed by two-way analysis of variance (ANOVA) followed by Bonferroni post hoc test. Data were expressed as mean  $\pm$  standard error of the mean and considered statistically significant when  $p$ -value was  $<0.05$ .

## **Results**

### *Hypoperfusion induces severe reductions in cerebral blood flow*

To determine if hypoperfusion induced reductions in cerebral blood flow, laser speckle contrast imaging was used one and seven days following surgery (supplemental Figure 1(a)). There was a significant effect of surgery ( $F_{(1,18)}=58.2$ ;  $p<0.0001$ ) and of time ( $F_{(2,36)}=51.6$ ;  $p<0.0001$ ) in the CBF values (% of baseline). Post hoc analysis showed that there is a significant reduction in CBF in hypoperfused mice compared with sham-treated mice 24 h ( $p<0.001$ ) and seven days following surgery ( $p<0.001$ ) (supplemental Figure 1(b)).

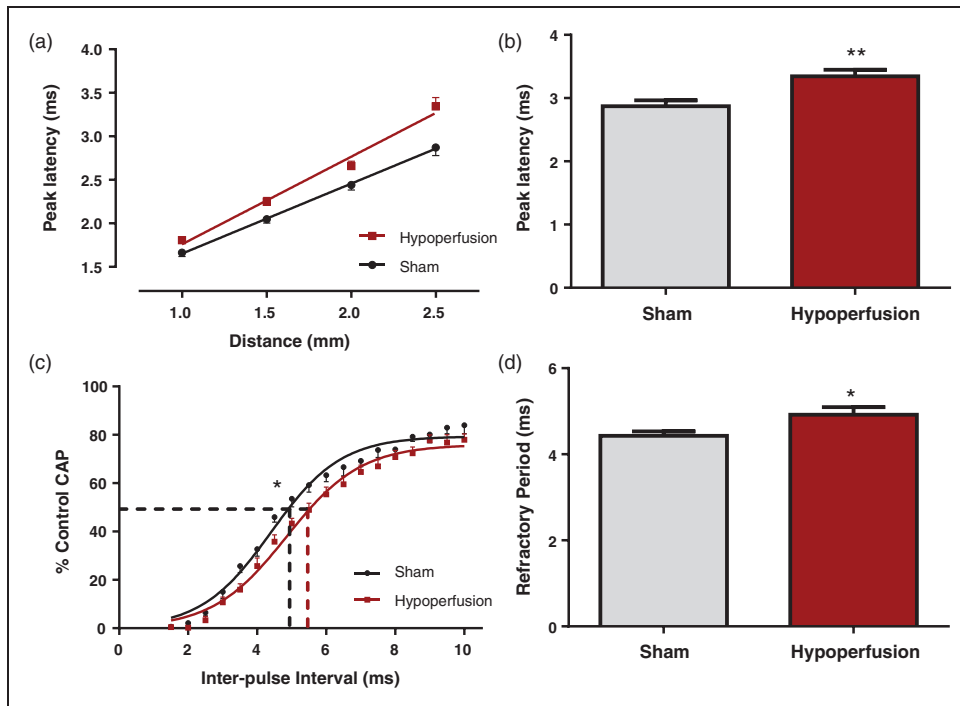


**Figure 1.** Deficits in white matter function in response to severe chronic hypoperfusion in myelinated fibres. (a, b) There was a significant increase in peak latency at 2.5 mm from the stimulating electrode (\*\* $p = 0.003$ ), indicative of slowed conduction of myelinated fibres, in hypoperfused animals. (c, d) For axonal refractoriness, the interpulse interval resulting in a 50% reduction in the CAP was significantly reduced in hypoperfused mice, indicative of perturbed axonal health (\* $p = 0.03$ ), when compared with sham-treated animals. Data are presented as mean  $\pm$  S.E.M. Student's  $t$  test, \* $p < 0.05$  \*\* $p < 0.01$ ,  $n = 12$  per group.

### Severe hypoperfusion induces a deficit in white matter function

At the outset, the effects of severe hypoperfusion on white matter function at seven days were assessed by electrophysiology in the corpus callosum. The peak latency of evoked CAPs, as an index of conduction velocity, was significantly increased in hypoperfused by  $17\% \pm 3.6\%$  as compared to sham mice ( $p = 0.003$ ) (Figure 1(a) and (b)). As a measure of axonal health, axonal refractoriness of CAPs was studied in the corpus callosum. The interpulse interval resulting in a 50% reduction in the CAP was significantly increased in hypoperfused mice, indicative of perturbed axonal health ( $p = 0.03$ ) when compared with sham-treated animals (Figure 1(c) and (d)). Collectively, these data indicate that callosal white matter fibres exhibit pronounced alterations in their electrophysiological properties in response to severe hypoperfusion.

### Increased white matter pathology and inflammation in response to severe hypoperfusion

To determine if the deficit in white matter function was accompanied by pathological changes to myelinated

axons and an inflammatory response, the adjacent slices to those used for electrophysiology were assessed. There was a significant reduction in the % area of MBP staining following hypoperfusion, indicating that hypoperfusion caused myelin pathology ( $p = 0.016$ ; Figure 2(a) and (b)). Axonal bulbs, detected with APP immunohistochemistry, were not present in sham-treated animals but were significantly increased in hypoperfused animals ( $p = 0.001$ ; Figure 2(c) and (d)), thus indicating that hypoperfusion caused axonal pathology.

Iba-1-positive immunostaining was undertaken in the corpus callosum to investigate the impact of hypoperfusion on inflammation (Figure 3(a)). There was a significant increase in the number of Iba-1-positive cells ( $p = 0.0003$ ; Figure 3(b)) and the density of Iba-1-immunostaining ( $p = 0.009$ ; Figure 3(c)) following hypoperfusion. A number of studies have indicated that pharmacological drugs which reduce microglia in white matter can improve conduction velocity,<sup>26,27</sup> suggesting that increased microglia may cause white matter dysfunction. We investigated this by correlating microglia/macrophages with peak latency or axonal refractoriness. There was a significant positive correlation between numbers

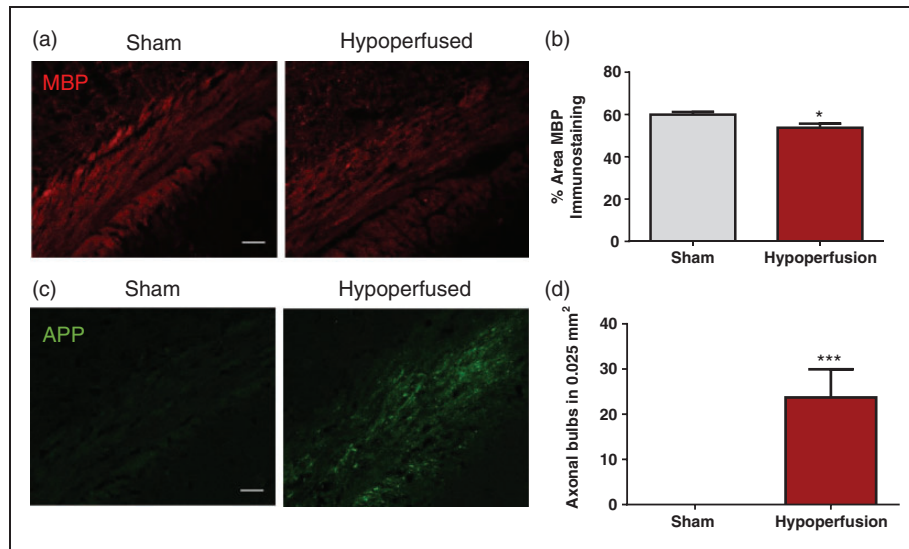


**Figure 2.** White matter pathology in response to severe chronic hypoperfusion. (a) Confocal images from the corpus callosum of animals immunostained with MBP (red), scale bar: 50  $\mu\text{m}$ . (b) There was a significant reduction in the % area of MBP immunostaining following hypoperfusion (\* $p = 0.016$ ). (c) Confocal images from the corpus callosum of animals immunostained with APP (green), scale bar: 50  $\mu\text{m}$ . (d) There was a significant increase in axonal damage following hypoperfusion (\*\*\* $p = 0.001$ ).

of microglia and slowing of peak latency ( $r = 0.59$ ,  $p = 0.002$ ; Figure 3(d)) and density of Iba-1 immunostaining and slowing of peak latency ( $r = 0.55$ ,  $p = 0.006$ ; Figure 3(e)), thus indicating an association between microglia/macrophages and deficits in conduction velocity. There was no significant association between microglial/macrophage numbers and slowing of axonal refractory period ( $r = 0.4$ ,  $p = 0.06$ ; Figure 3(e)) or microglial/macrophage density and slowing of axonal refractory period ( $r = 0.29$ ,  $p = 0.17$ ; Figure 3(g)).

#### DMF treatment improves white matter function following severe hypoperfusion

To further investigate the hypothesis that microglia can cause white matter dysfunction, a drug which is known to reduce microglial activation, DMF,<sup>36</sup> was investigated to determine if it could protect improve white matter function following hypoperfusion. DMF significantly reduced the peak latency in hypoperfused mice by  $7\% \pm 1.2\%$  of vehicle-treated hypoperfused mice control values ( $p < 0.05$ ) (Figure 4(a) and (b)). Thus, the data indicate a beneficial effect of DMF on conduction velocity of myelinated fibres. Axonal refractoriness was not significantly altered by DMF treatment ( $p = 0.07$ ) (Figure 4(c) and (d)). Therefore, these data indicate that callosal white matter fibres exhibit pronounced alterations in conduction velocity and that DMF treatment can improve white matter function.

#### Hypoperfusion causes a breakdown of axon-glia integrity that is unaffected by DMF

Following the demonstration that DMF improved white matter function in hypoperfused mice, its impact on hypoperfusion-induced pathology to myelinated axons was explored. MBP, a marker of myelin integrity, was not significantly altered in response to hypoperfusion or DMF administration (Figure 5(a) and (b)). Therefore, a further marker of myelin damage was investigated, MAG, as reductions in MAG intensity have been demonstrated previously in response to hypoperfusion, indicative of altered axon-glia integrity.<sup>9,14</sup> A significant reduction in MAG immunostaining was determined following severe hypoperfusion ( $F_{(1-33)} = 11.7$ ;  $p = 0.002$ ), but there was no significant effect of DMF administration or interactions (Figure 4(c) and (d)). Post hoc comparison showed a significant reduction in MAG immunostaining with hypoperfusion in both vehicle- ( $p < 0.05$ ) and DMF-treated ( $p < 0.05$ ) groups when compared with sham controls.

Previous studies have revealed differential vulnerabilities of mature oligodendrocytes and their precursor cells in response to hypoperfusion. Oligodendrocytes have been suggested to facilitate axonal conduction by mechanisms other than myelination.<sup>45</sup> Thus, the numbers of these cells were determined after hypoperfusion and DMF treatment using CC1 and NG2 immunohistochemistry for mature oligodendrocytes and OPCs, respectively (Figure 5(e)). Although there was a significant reduction in the number of CC1-positive

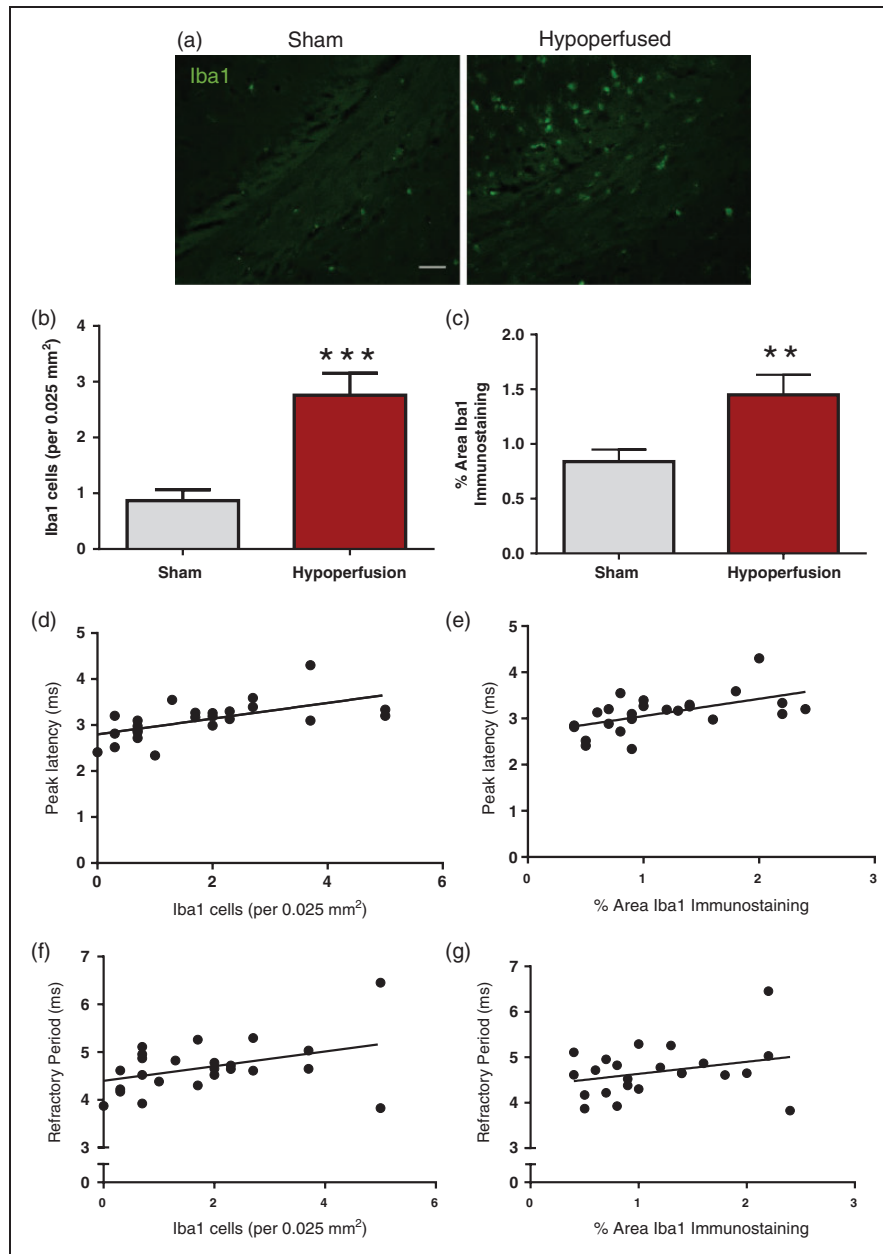


**Figure 3.** Elevated microglia/macrophage number and density in response to severe chronic hypoperfusion. (a) Confocal images from the corpus callosum of animals immunostained with Iba1 (green), scale bar: 50  $\mu\text{m}$ . (b) There was a significant increase in microglial numbers following hypoperfusion ( $***p = 0.0003$ ). (c) There was a significant increase in % area of Iba1 immunostaining following hypoperfusion ( $**p = 0.009$ ). (d) There was a significant positive correlation between numbers of microglia and slowing of peak latency ( $r = 0.59$ ,  $p = 0.002$ ). (e) There was a significant positive correlation between % area of Iba1 immunostaining and peak latency ( $r = 0.55$ ,  $p = 0.006$ ). (f) There was no significant association between microglial numbers and slowing of axonal refractory period ( $r = 0.4$ ,  $p = 0.06$ ) (g) and no association between % area of Iba1 immunostaining and peak latency ( $r = 0.29$ ,  $p = 0.17$ ). Data are presented as mean  $\pm$  S.E.M. Student's *t* test,  $*p < 0.05$   $**p < 0.01$ ,  $***p < 0.001$ ;  $n = 12$  per group.

cells ( $F_{(1,31)} = 13.0$ ,  $p = 0.001$ ) in response to hypoperfusion, DMF treatment had no effect and there were no significant interactions (Figure 4(f)). Post hoc comparison indicated a significant reduction in the number of CC1 immunopositive cells following hypoperfusion in DMF-treated mice ( $p < 0.05$ ) but not in vehicle-

treated mice ( $p > 0.05$ ). In contrast, there was a significant increase in the number of NG2-positive cells ( $F_{(1,33)} = 7.6$ ,  $p = 0.009$ ); however, DMF treatment had no significant effect on the number of NG2 cells and there were no significant interactions (Figure 5(f)).



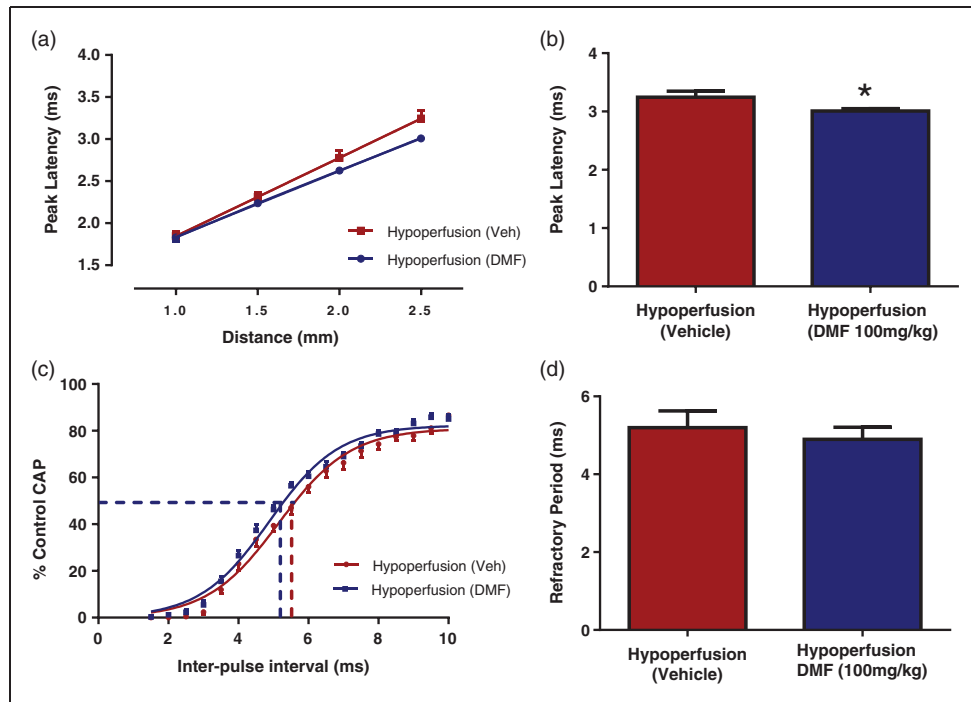


**Figure 4.** DMF treatment improved the peak latency of CAP, but not axonal refractoriness following severe chronic hypoperfusion. (a, b) DMF-treated hypoperfused mice had a reduced peak latency compared to vehicle-treated mice (\* $p < 0.05$ ) indicating that DMF is able to improve conduction velocity of myelinated fibres. (c, d) Axonal refractoriness was not significantly altered by DMF treatment ( $p = 0.07$ ). Data are presented as mean  $\pm$  S.E.M. Student's  $t$  test, \* $p < 0.05$   $n = 12$  per group.

To build on the previous findings that axonal health was impaired by hypoperfusion but axonal refractoriness was not modulated by DMF, axonal pathology was investigated by APP immunostaining and assessment of the number of APP-positive axonal bulbs (Figure 5(g)). Axonal bulbs were not detected in sham mice but were observed in hypoperfused mice in the corpus callosum. There was a significant increase in the number of APP-positive axonal bulbs after hypoperfusion surgery ( $F_{(1-33)} = 4.9$ ,  $p = 0.04$ ), but the number was unaffected by DMF and there were no significant interactions (Figure 5(h)).

Thus, although hypoperfusion causes damage to myelinated axons, axon-glia integrity and the number of mature and immature oligodendrocytes, these measures were unaffected by DMF.

#### *Hypoperfusion increased microglial/macrophage density which is modulated by DMF*

Previous studies have indicated that DMF may exert protective effects through inflammatory mechanisms.<sup>32,36</sup> Since we found a significant association between microglia/macrophages and deficits in white matter function, we next determined if microglial/macrophages would be affected by DMF treatment (Figure 6(a)). Microglial/macrophage density was

significantly increased following hypoperfusion ( $F_{(1-33)} = 7.93$ ,  $p = 0.008$ ), but there was no effect of drug treatment (Figure 6(b)). Notably, post hoc analysis showed that there was a significant increase in Iba1 staining in hypoperfused vehicle-treated mice compared with sham vehicle-treated mice ( $p < 0.05$ ), but there was no difference between sham and hypoperfused mice treated with DMF ( $p > 0.05$ ), suggesting that DMF modestly reduced the density of microglia/macrophages.

#### *Hypoperfusion and DMF treatment effects on cytokines, chemokines and growth factors*

The modest reduction in the microglial/macrophage response to hypoperfusion with DMF treatment suggested that DMF may act by modulating levels of inflammatory-related proteins. To further explore neuroinflammatory mechanisms, a range of cytokines, chemokines and growth factors were examined using a multiplex immunoassay.

The levels of chemoattractant and growth factor molecules MIP-1 $\alpha$ , MCP-1, KC and VEGF were examined firstly (Figure 7). All four molecules were significantly increased after hypoperfusion (MIP-1 $\alpha$   $F_{(1-34)} = 13.7$ ,  $p = 0.0008$ ; MCP-1  $F_{(1-34)} = 18.2$ ,  $p = 0.0001$ ; KC  $F_{(1-33)} = 14.3$ ,  $p = 0.0006$ ; VEGF  $F_{(1-34)} = 34.8$ ,

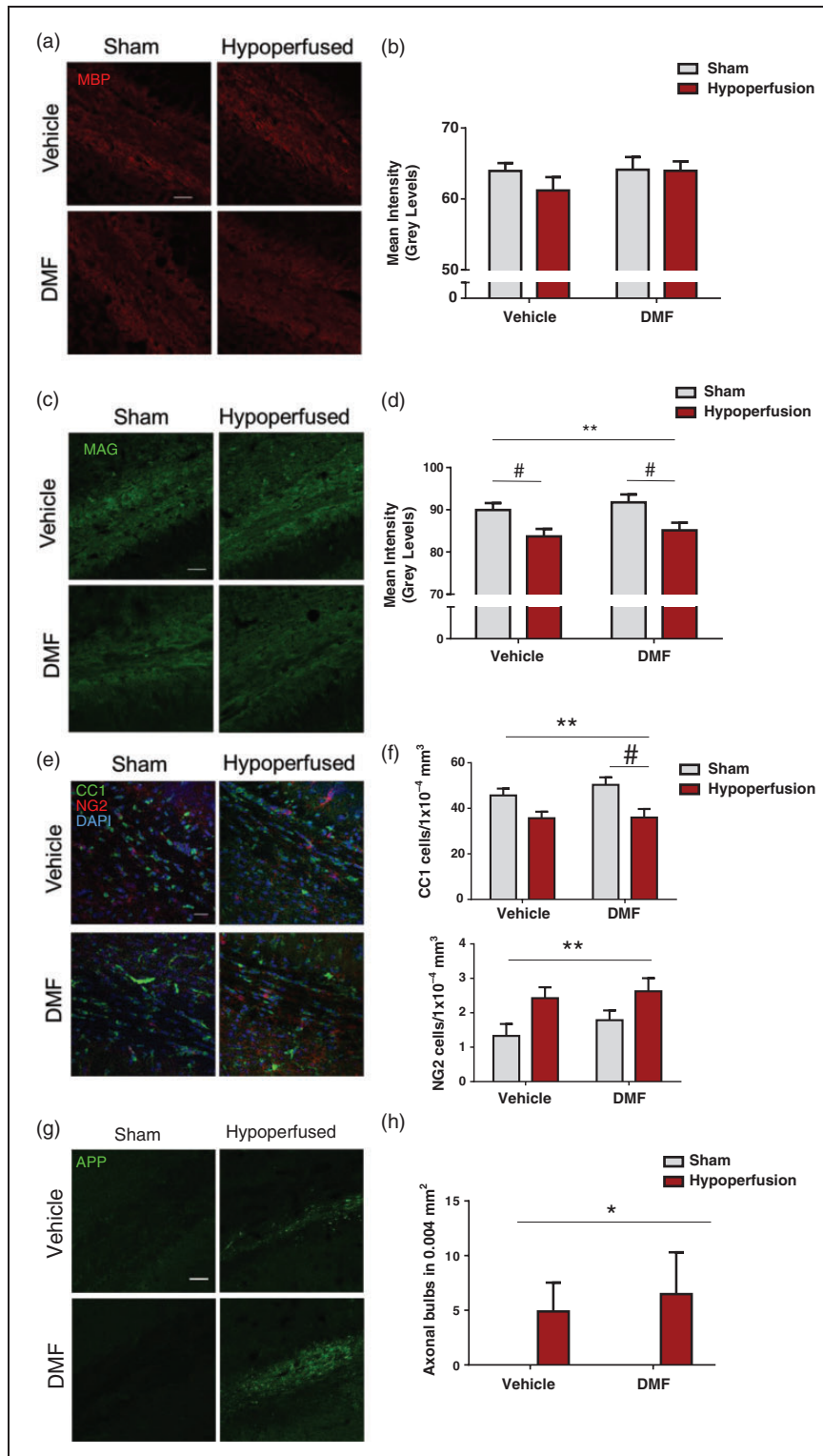


**Figure 5.** Axon-glia integrity was damaged by severe hypoperfusion but unaffected by DMF administration. (a) Confocal images from the corpus callosum of animals from four experimental groups immunostained with MBP (red), scale bar: 50  $\mu$ m. (b) Quantification of MBP immunostaining sections showing no significant changes in myelin among the groups. (c) Confocal images from the corpus callosum of animals from four experimental groups immunostained with MAG (green), scale bar: 50  $\mu$ m. (d) MAG immunostained sections showing changes in myelin in hypoperfused animals. Quantification of MAG mean intensity shows an overall significant effect of surgery ( $F_{(1,31)} = 11.7$ ;  $**p = 0.002$ ) Post hoc comparison shows a significant reduction with hypoperfusion in both

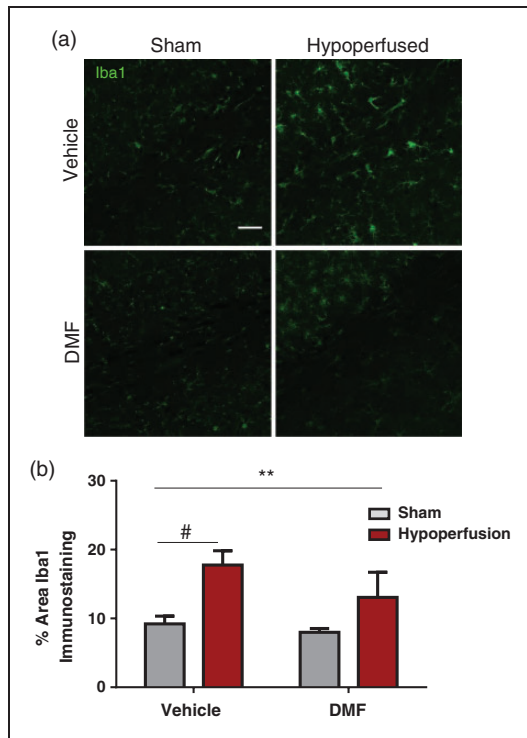


**Figure 6.** The effect of DMF on the microglial response. (a) Confocal images from the corpus callosum from four experimental groups. Green: Iba1; Scale bar: 50  $\mu$ m. (b) There was a significant effect of surgery ( $F_{(1,33)} = 7.9$ ;  $**p = 0.008$ ) in the % area of Iba1 immunostaining. Notably, post hoc analysis showed that there is a significant increase in Iba1 staining in hypoperfused vehicle treated mice compared with sham vehicle treated mice ( $\#p < 0.05$ ), but no difference between sham and hypoperfused mice treated with DMF ( $p > 0.05$ ). Data are presented as mean  $\pm$  SEM, Two-way ANOVA followed by Bonferroni post hoc test, sham vehicle  $n = 7$ ; sham DMF  $n = 8$ ; hypoperfusion vehicle  $n = 13$ ; hypoperfusion DMF  $n = 9$ .

$p < 0.0001$ ), and there was no significant effect of DMF administration or significant interactions. Post hoc comparison showed a significant increase in the levels of MCP-1, KC and VEGF in hypoperfused vehicle-treated mice compared with sham vehicle-treated mice and in DMF hypoperfused compared to DMF sham-treated mice. In contrast, although MIP-1 $\alpha$  levels were

significantly increased ( $p < 0.01$ ) in hypoperfused vehicle-treated mice compared with sham vehicle-treated mice, MIP-1 $\alpha$  levels in DMF-treated hypoperfused mice were not significantly different compared with sham DMF-treated mice ( $p > 0.05$ ) suggesting that DMF reduced levels of MIP-1  $\alpha$  (Figure 7(a)).

Three cytokines were examined, IL-6, IL-1 $\beta$  and IFN- $\gamma$  (Figure 7). IL-6 levels were significantly increased after hypoperfusion ( $F_{(1,34)} = 4.4$ ,  $p = 0.04$ ) but unaffected by DMF treatment, and there were no significant interactions (Figure 7(e)). IL-1  $\beta$  and IFN- $\gamma$  were unaffected by hypoperfusion surgery or DMF treatment (Figure 7(f) and (g)).

Therefore, overall analyses indicated hypoperfusion had a prominent effect on inflammatory-related molecules which was unaffected by DMF treatment except for MIP 1 $\alpha$  levels which were dampened by DMF treatment.

## Discussion

The present study demonstrated that severe hypoperfusion induces a deficit in white matter function in the corpus callosum which is correlated with a marked increase in microglia/macrophages. Treatment with an anti-inflammatory drug, DMF, improved white matter function and dampened microglial/macrophage density induced by severe hypoperfusion.

White matter function assessed with electrophysiology was markedly impaired in the corpus callosum, key tracts connecting cerebral hemispheres and vulnerable to damage following chronic hypoperfusion.<sup>8,15</sup> The assessment of evoked CAPs has been used in a number of other studies to demonstrate that perturbations in white matter can impact their function. For example, deficits in white matter function have been detected by measuring CAP in response to oxygen glucose deprivation,<sup>46-48</sup> TBI<sup>49</sup> and excitotoxicity.<sup>50</sup> This approach is very sensitive to the electrophysiological properties of white matter and can be used to detect altered function caused by subtle alterations of white matter such as differing effect of sex hormone on recovery from cuprizone demyelination<sup>51,52</sup> and glutathione depletion.<sup>53</sup>

### Figure 5. Continued

vehicle ( $\#p < 0.05$ ) and DMF treated ( $\#p < 0.05$ ) groups. (e) Confocal images from the corpus callosum from four experimental groups immunostained for markers of mature oligodendrocytes (CC1) and oligodendrocyte precursor cells (NG2). Green: CC1; red: NG2, blue: DAPI, scale bar: 100  $\mu$ m. (f) There is a significant reduction in the number of CC1 cells following hypoperfusion ( $F_{(1,33)} = 13.0$ ;  $**p = 0.001$ ) Post hoc comparison shows a significant reduction in the number of CC1 immunopositive cells following hypoperfusion in DMF-treated mice ( $\#p < 0.05$ ) but not in vehicle-treated mice ( $\#p > 0.05$ ). There was significant increase in NG2-positive cells following hypoperfusion surgery ( $F_{(1,33)} = 7.6$ ;  $**p = 0.009$ ). (g) APP-immunostained sections showing axonal damage in hypoperfused animals while minimal immunostaining is detected in shams. Green: APP. Scale bar: 50  $\mu$ m. (h) Quantification of axonal bulbs shows an overall significant effect of surgery ( $F_{(1,33)} = 4.9$ ;  $*p = 0.04$ ). Data presented as mean  $\pm$  SEM, Two-way ANOVA followed by Bonferroni post hoc test, sham vehicle  $n = 7$ ; sham DMF  $n = 8$ ; hypoperfusion vehicle  $n = 13$ ; hypoperfusion DMF  $n = 9$ .

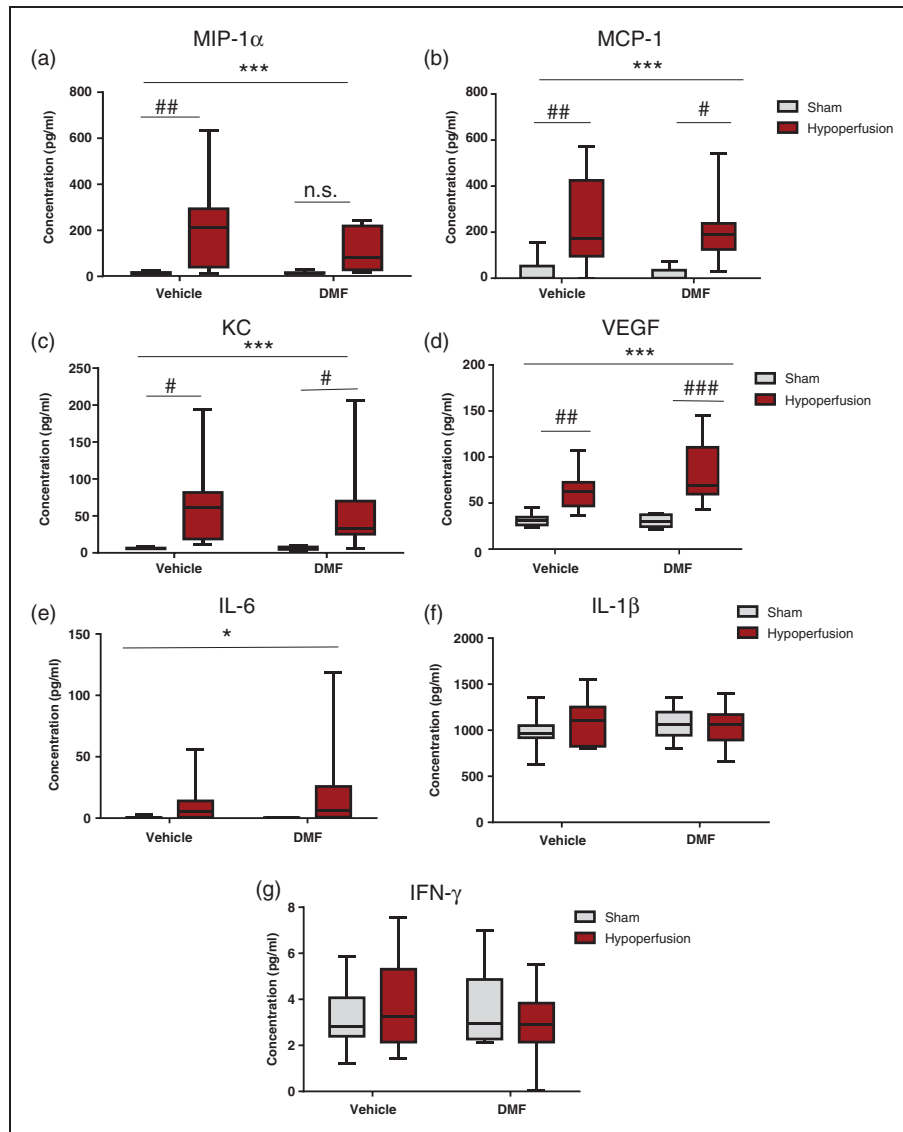


**Figure 7.** The effect of DMF on chemokines, growth factors and cytokines. Levels of inflammatory-related proteins were calculated (pg/ml) using a multiplex assay. (a) There was a highly significant effect of surgery ( $F_{(1-34)} = 13.7$ ;  $***p = 0.0008$ ) in the concentration of MIP-1 $\alpha$  (pg/ml). Post hoc analysis showed that there was a significant increase in MIP-1 $\alpha$  levels in hypoperfused vehicle-treated animals compared with sham vehicle-treated animals ( $###p < 0.01$ ); however, notably there was no significant increase in MIP-1 $\alpha$  levels in the DMF-treated hypoperfused mice compared with sham mice ( $p > 0.05$ ). (b) There was a highly significant effect of surgery ( $F_{(1-34)} = 18.2$ ;  $***p = 0.0001$ ) in the concentration of MCP-1 (pg/ml). Post hoc analysis showed that there was a significant increase in MCP-1 levels in hypoperfused vehicle-treated animals compared with sham vehicle-treated animals ( $###p < 0.01$ ) and a significant increase in MCP-1 levels in hypoperfused DMF-treated animals compared with sham DMF-treated animals, but by a lesser magnitude ( $#p < 0.05$ ). (c) There was a significant effect of surgery ( $F_{(1-33)} = 14.3$ ;  $***p = 0.0006$ ) in the concentration of KC (pg/ml). Post hoc analysis showed that there was a significant elevation in KC levels following hypoperfusion vehicle compared with sham vehicle treatment ( $#p < 0.05$ ), and in hypoperfused DMF-treated mice when compared with sham DMF-treated mice ( $#p < 0.05$ ). (d) There was a highly significant effect of surgery ( $F_{(1-34)} = 34.8$ ;  $***p < 0.0001$ ) in the concentration of VEGF (pg/ml). Post hoc analysis showed that there was a significant increase in VEGF levels in hypoperfused vehicle-treated animals compared with sham vehicle-treated animals ( $###p < 0.01$ ). Notably, there was also a significant increase in VEGF levels in the DMF-treated hypoperfused mice compared with the DMF-treated sham mice, by a greater magnitude ( $####p < 0.001$ ) than the increase seen in vehicle treated mice. (e) For IL-6 levels, there was a significant effect of surgery ( $F_{(1-34)} = 4.4$ ,  $*p = 0.04$ ). (f and g) There was no significant effect of hypoperfusion or DMF for IL-1 $\beta$  (f) or for IFN- $\gamma$  (g). Data are presented as mean  $\pm$  SEM, two-way ANOVA followed by Bonferroni post hoc test, sham vehicle  $n = 8$ ; sham DMF  $n = 8$ ; hypoperfusion vehicle  $n = 11$ ; hypoperfusion DMF  $n = 11$ .

The deficits in white matter function induced by hypoperfusion included a slowing of peak latency of CAP, indicative of slowed conduction velocity. Conduction velocity is the rate at which a nerve impulse is propagated, and is dependent on normal myelination. Similar slowing of conduction velocity has been demonstrated following low-level blast trauma,<sup>54</sup> demyelination<sup>44</sup> and neonatal hyperoxia.<sup>55</sup> We also demonstrated that severe hypoperfusion increased the axonal refractory period, indicative of perturbed axonal health. Increased refractory period has been reported after hypoxia in spinal cord; however, this could be recovered following re-oxygenation, suggesting that hypoxia may be a key mechanism of increased refractoriness following hypoperfusion.<sup>56</sup> Demyelination of axons induced by cuprizone or TBI and compression injury also cause increases in refractoriness.<sup>44,49,57,58</sup>

Severe hypoperfusion resulted in white matter pathology, including myelin and axonal damage detected with MBP and APP immunohistochemistry that may account for the deficits in white matter function. This is an agreement with other studies where structural alterations in white matter are reported to underlie functional alterations. For example, demyelination or myelin thinning and axonal damage, detected with electron microscopy or APP immunohistochemistry, are present in white matter following cuprizone demyelination, TBI or excitotoxicity which resulted in reduced CAP amplitude, conduction velocity and increased refractoriness.<sup>43,44,49,50,57</sup>

We found a significant elevation in microglia/macrophages in the corpus callosum following severe hypoperfusion. Microglial activation is a robust response to reduced cerebral blood flow following chronic hypoperfusion<sup>8,14</sup> and in stroke models.<sup>59,60</sup> Furthermore, there was a positive correlation between microglia/macrophages and slowing of peak latency, suggesting that the elevated inflammatory environment in myelinated axon tracts may contribute to the functional deficit. Increased microglial levels are also reported in white matter that exhibit deficits in conduction velocity or refractoriness following cuprizone demyelination,<sup>44</sup> EAE<sup>61</sup> or TBI.<sup>58</sup> The extent of axonal damage in demyelinating MS lesions is associated with increased numbers of activated microglia/macrophages<sup>62</sup> which have been hypothesised to play a mechanistic role in white matter damage through the release of inflammatory-related mediators such as nitric oxide, which can induce reversible conduction block and axonal degeneration in demyelinated axons.<sup>63</sup>

To further test the hypothesis that microglia may mediate the deficits in white matter function, we used a drug, DMF, which is known to reduce microgliosis in a number of disease models including focal cerebral ischaemia.<sup>36,64</sup> DMF was found to significantly

improve peak latency following severe hypoperfusion. This corroborates with other studies which have shown that DMF can exert protective effects on motor and neurological function in focal cerebral ischaemia,<sup>36,64</sup> intracerebral haemorrhage<sup>35</sup> and other models of neurodegeneration.<sup>29,31,32,41,65</sup> DMF is also known to protect against cognitive deficits assessed in the Morris water maze in a mouse model of subarachnoid haemorrhage.<sup>34</sup> MMF (derivative of DMF) protects against functional deficits assessed with electrophysiology in retinal ischaemia-reperfusion<sup>66</sup> and in an experimental autoimmune neuritis model.<sup>65</sup>

Although DMF exerted protective effects on white matter function in the corpus callosum, this was not paralleled by protective effects on white matter structure. In a first cohort, reduced MBP immunostaining was determined in mice that exhibited functional deficits following hypoperfusion, confirming the findings of Miki et al.<sup>15</sup> in severe hypoperfusion. However, in a second cohort, a similar reduction in MBP staining was not found. The reasons for these differences between cohorts are not clear. One explanation may be that the tissue was processed differently using sucrose treatment and cryostat sectioning as opposed to paraffin embedding. To further examine myelin integrity after hypoperfusion, we therefore used another marker, MAG which we previously demonstrated to be sensitive to chronic hypoperfusion.<sup>9,14</sup> However, despite the reductions in MAG immunostaining in response to severe hypoperfusion, MAG pathology was not attenuated with DMF. Oligodendrocytes contain a number of ion channels and neurotransmitter receptors which monitor neuronal activity and facilitate axonal conduction by mechanisms other than myelination.<sup>45</sup> Therefore, in light of the fact that DMF did not modulate MAG pathology, we examined the effects of DMF on mature and immature oligodendrocyte populations. We demonstrated that mature oligodendrocytes are particularly vulnerable to hypoperfusion with levels markedly reduced seven days following hypoperfusion. This finding is in agreement with our previous study<sup>14</sup> and that of others<sup>18</sup> indicating CC1 levels are reduced within days following chronic hypoperfusion and focal cerebral ischemia.<sup>67,68</sup> In contrast, the levels of NG2 oligodendrocyte cells were increased in response to severe hypoperfusion, as others<sup>69</sup> have reported following focal cerebral ischaemia. However, there was no protective effect of DMF administration on oligodendrocyte numbers after hypoperfusion. Similarly, DMF has no protective effects on mature and oligodendrocyte precursor cells following cuprizone demyelination.<sup>70</sup>

Collectively, the data indicate that DMF can improve white matter function following hypoperfusion, but this is not associated with a concomitant

protective effect on axonal-glial integrity. A multitude of factors contribute to conduction velocity along myelinated fibres which also include the distribution and density of ion channels at nodal regions. Other studies have showed that deficits in conduction velocity and axonal refractoriness are sustained in the recovery from neonatal hyperoxia or withdrawal from cuprizone diet,<sup>44,55</sup> despite a recovery of axon-glial integrity. Instead, they found sustained, subtle alterations in the structural composition of the paranode and Node of Ranvier including increased spread of Nav1.6 channels along the Node of Ranvier, which we have also reported after mild chronic hypoperfusion.<sup>9</sup> Clofazimine, a drug which prevents loss of potassium channels, can improve conduction velocity and axonal refractoriness following TBI.<sup>58</sup> Therefore, the limited exploration of axon-glial integrity that we have carried out may not be the most sensitive pathological indices of functional deficits, and instead specific regions of node and paranodal domains of myelinated axons and ion channels may be vulnerable.

An important consideration of the present study is whether the dose of DMF was appropriate to ensure maximal protective effects in white matter. Protective effects of DMF have been reported at doses as low as 15 mg/kg in intracerebral/subarachnoid haemorrhage and EAE<sup>33,34,40</sup> and 30 mg/kg in a model of Huntington's disease.<sup>29</sup> More recently, Schulze-Topoff et al.<sup>42</sup> used the same dose as the present study (100 mg/kg) to demonstrate clinical and histological protection following EAE. DMF is thought to act mechanistically by enhancing the activity of Nrf2 signalling, an endogenous survival pathway with anti-oxidant and anti-inflammatory effects. Nrf2 is a transcription factor that activates a battery of cytoprotective genes such as genes encoding heme-oxygenase-1 (*hmx1*), *osgin 1* (*osgin 1*) and NAD(P)H dehydrogenase quinone 1 (*nqo1*). Brennan et al.<sup>71</sup> recently carried out an investigation of the dose-response effect of DMF on Nrf2-dependent gene changes. For many genes studied, such as *hmx1*, there were no notable increases in the brain following 100 mg/kg of DMF; however, 400 and 600 mg/kg could induce increases in *hmx1* expression, an effect reported by others.<sup>32</sup> Therefore, it may be possible that the modest protective effects that DMF (100 mg/kg) had on white matter function in the present study could be enhanced with a higher dosage.

In contrast to the protective effects of DMF on peak latency, we found no parallel protective effects on axonal refractoriness, as an index of axonal health. Similarly, we found a significant increase in APP immunostaining, indicative of axonal damage, following severe chronic hypoperfusion that was not attenuated with DMF treatment. Similar results were reported on

white matter function following administration of the immunophilin ligand FK506 after TBI. FK506 treatment could protect against deficits in CAP amplitude, but did not reduce refractory changes in myelinated fibres.<sup>72</sup> DMF has been reported to protect against axonal damage detected with APP immunohistochemistry in EAE<sup>41</sup> and EAN;<sup>73</sup> however, this may reflect a different disease mechanism.

Although we did not detect protective effects of DMF on hypoperfused-induced damage to myelinated axons, we found that DMF led to modest reductions in the extent of microglial/macrophage density. There is a marked reduction in microglial levels in vivo following DMF treatment in a mouse model of synucleinopathy<sup>32</sup> and Parkinson's disease.<sup>31</sup> Of relevance to the current study, DMF was found to significantly reduce microglial levels following focal cerebral ischaemia,<sup>36</sup> an effect that was paralleled by reduced cytokine levels.<sup>64</sup> In support of our hypothesis that reductions in microglia/macrophages can improve white matter function, HDAC inhibition or the sodium channel blocker safinamide reduced pro-inflammatory microglia/macrophages and improved CAP amplitude in the corpus callosum following TBI or EAE.<sup>26,27</sup> One limitation of the current study is that the Iba-1 immunostaining cannot discriminate between macrophages and brain-derived microglia; therefore, some of the immunostaining may represent infiltration of peripheral-derived macrophages. Indeed, transient blood-brain barrier disruption has been reported in white matter in a rat model of chronic cerebral hypoperfusion<sup>74</sup> and may contribute to the functional deficit in the present study. In support of this, it has been reported that DMF can protect the blood-brain barrier following focal cerebral ischaemia in the mouse<sup>75</sup> via decreased matrix metalloproteinase activity and protection of interendothelial tight junctions, resulting in reduced brain oedema. This raises the possibility that the beneficial effects of DMF on white matter function that we have reported may have been partly mediated through protection of the blood-brain barrier, particularly given the modest effects of DMF on inflammation that we found.

DMF has been shown to inhibit microglial inflammation in vitro and to suppress the expression of pro-inflammatory cytokines.<sup>76</sup> Therefore, to further investigate the modulation of inflammatory-related proteins after severe hypoperfusion and DMF treatment, a panel of molecules were investigated with multiplex. The chemoattractant molecules MIP-1 $\alpha$  (CCL3) and MCP-1 (CCL2) are both upregulated in the present study, and are also upregulated in response to focal cerebral ischaemia and chronic hypoperfusion.<sup>77-79</sup> These chemokines regulate the infiltration of monocytes/macrophages into the CNS under pathological

conditions and are associated with exacerbating neuronal damage,<sup>80</sup> whereas their inhibition protects neurons.<sup>81</sup> We have reported that MIP-1 $\alpha$  levels are modestly dampened following DMF administration, and this may contribute to the protective effect of DMF on white matter function, possibly via effects on monocyte/macrophage infiltration from the periphery. Lin et al.<sup>64</sup> reported that DMF reduced the number of MPO+neutrophils and CD3+T cells which infiltrated the penumbral region following focal cerebral ischaemia.

Levels of the growth factor VEGF were increased in response to severe chronic hypoperfusion. VEGF is associated with protective effects following focal cerebral ischaemia and chronic cerebral hypoperfusion, including neuroprotection, increased angiogenesis and cerebral blood flow.<sup>82,83</sup> Of interest, Wiesner et al.<sup>84</sup> showed that VEGF levels are elevated in astrocyte cultures treated with DMF, mediated by Nrf2 signalling.

Of the three cytokines that were assessed in the current study, only IL-6 was found to be significantly increased seven days following chronic hypoperfusion. IL-6 is reported to have both pro- and anti-inflammatory effects;<sup>85</sup> however, in the context of cerebral hypoperfusion, it confers neuroprotective effects.<sup>86</sup> However, we did not find evidence that DMF altered IL-6 levels. In contrast to the increase in IL-6 we have reported, the cytokines IL-1 $\beta$  and IFN- $\gamma$  were not altered in response to chronic hypoperfusion or DMF treatment. IL-1 $\beta$  is increased after focal cerebral ischaemia<sup>87</sup> and promotes neuronal damage. Although we did not detect any alterations in IL-1 $\beta$ , others have reported that levels of IL-1 $\beta$  appear to alter transiently at different time points in response to differing extents of cerebral hypoperfusion.<sup>16,88</sup> We also reported no alterations in IFN- $\gamma$  levels, which concurs with findings in focal cerebral ischaemia.<sup>89</sup> Collectively, there was minimal evidence that DMF could modulate cytokine levels, whereas modest effects were seen on MIP-1 $\alpha$ .

Given the modest protective effects of DMF that we have reported seven days following severe hypoperfusion, it would be interesting to study longer term time points. Miki et al.<sup>15</sup> showed that severe hypoperfusion causes progressive white matter pathology and we have previously reported that more modest decreases in cerebral blood flow cause increased microgliosis and altered axon-glial integrity at one month,<sup>8,9</sup> that progresses to include microinfarcts, haemorrhage and blood-brain barrier alterations. DMF is reported to reduce ischaemic neuronal death, oedema and blood-brain barrier breakdown<sup>36,64,75</sup> in the acute response to focal cerebral ischaemia thus may have protective effects in the chronic response to modest blood flow reduction. DMF is reported to have protective effects following

long-term administration in EAE,<sup>40,41</sup> Parkinson's disease,<sup>32</sup> and following one year of administration in a mouse model of Huntington's disease.<sup>29</sup>

To conclude, we have demonstrated that severe hypoperfusion caused deficits in white matter function and that DMF improved white matter function following severe hypoperfusion. Although there was no effect of DMF on the structural integrity of damaged myelinated axons, DMF had modest effects on microglia/macrophages.

## Funding

The author(s) disclosed receipt of the following financial support for the research, authorship, and/or publication of this article: This work was supported by the Alzheimer's Society, Alzheimer Research UK, Biogen, Wellcome Trust and The University of Edinburgh Centre for Cognitive Aging and Cognitive Epidemiology (CCACE), part of the Lifelong Health and Wellbeing Initiative (G0700704/84698). J.M. was supported by a CCACE PhD studentship, J.H.F. was funded by an Alzheimer's Society Fellowship (Grant 297) and is currently funded by an Alzheimer's Research UK Senior Fellowship (Grant ARUK-SRF2013-4).

## Declaration of conflicting interests

The author(s) declared the following potential conflicts of interest with respect to the research, authorship, and/or publication of this article: At the time this work was performed, R.H.S. was an employee of and held stock/stock options in Biogen.

## Authors' contributions

J.H.F., J.M., P.R.H., Y.M., M.M., F.S., E.C. and K.H. performed experiments. J.H.F., J.M., R.H.S., G.E.H. and K.H. designed the experiments. J.H.F. and K.H. wrote the manuscript. J.M., P.R.H., Y.M., M.M., R.H.S. and G.E.S. provided critical feedback and contributed to drafting the manuscript together with the corresponding authors.

## Supplementary material

Supplementary material for this paper can be found at the journal website: <http://journals.sagepub.com/home/jcb>

## References

1. Wang Y, Liu G, Hong D, et al. White matter injury in ischemic stroke. *Prog Neurobiol* 2016; 141: 45–60.
2. Pantoni L, Garcia JH and Gutierrez JA. Cerebral white matter is highly vulnerable to ischemia. *Stroke* 1996; 27: 1641–1646. (discussion 7).
3. Petitto CK, Olarte JP, Roberts B, et al. Selective glial vulnerability following transient global ischemia in rat brain. *J Neuropathol Exp Neurol* 1998; 57: 231–238.
4. Matute C and Ransom BR. Roles of white matter in central nervous system pathophysiology. *ASN Neuro* 2012; 4: 89–101.

5. Fernando MS, Simpson JE, Matthews F, et al. White matter lesions in an unselected cohort of the elderly: molecular pathology suggests origin from chronic hypoperfusion injury. *Stroke* 2006; 37: 1391–1398.
6. Prins ND and Scheltens P. White matter hyperintensities, cognitive impairment and dementia: an update. *Nat Rev Neurol* 2015; 11: 157–165.
7. Holland PR, Bastin ME, Jansen MA, et al. MRI is a sensitive marker of subtle white matter pathology in hypoperfused mice. *Neurobiol Aging* 2011; 32: 2325.e1–6.
8. Coltman R, Spain A, Tsenkina Y, et al. Selective white matter pathology induces a specific impairment in spatial working memory. *Neurobiol Aging* 2011; 32: 2324.e7–12.
9. Reimer MM, McQueen J, Searcy L, et al. Rapid disruption of axon-glia integrity in response to mild cerebral hypoperfusion. *J Neurosci* 2011; 31: 18185–18194.
10. De Groot JC, De Leeuw FE, Oudkerk M, et al. Periventricular cerebral white matter lesions predict rate of cognitive decline. *Ann Neurol* 2002; 52: 335–341.
11. Prins ND, van Dijk EJ, den Heijer T, et al. Cerebral small-vessel disease and decline in information processing speed, executive function and memory. *Brain* 2005; 128: 2034–2041.
12. Holland PR, Searcy JL, Salvadores N, et al. Gliovascular disruption and cognitive deficits in a mouse model with features of small vessel disease. *J Cereb Blood Flow Metab* 2015; 35: 1005–1014.
13. Tekkok SB and Goldberg MP. Ampa/kainate receptor activation mediates hypoxic oligodendrocyte death and axonal injury in cerebral white matter. *J Neurosci* 2001; 21: 4237–4248.
14. McQueen J, Reimer MM, Holland PR, et al. Restoration of oligodendrocyte pools in a mouse model of chronic cerebral hypoperfusion. *PLoS One* 2014; 9: e87227.
15. Miki K, Ishibashi S, Sun L, et al. Intensity of chronic cerebral hypoperfusion determines white/gray matter injury and cognitive/motor dysfunction in mice. *J Neurosci Res* 2009; 87: 1270–1281.
16. Hou X, Liang X, Chen JF, et al. Ecto-5'-nucleotidase (CD73) is involved in chronic cerebral hypoperfusion-induced white matter lesions and cognitive impairment by regulating glial cell activation and pro-inflammatory cytokines. *Neuroscience* 2015; 297: 118–126.
17. Shi H, Zheng K, Su Z, et al. MCP-1 mediated activation of microglia promotes white matter lesions and cognitive deficits by chronic cerebral hypoperfusion in mice. *Mol Cell Neurosci* 2016; 78: 52–58.
18. Miyamoto N, Maki T, Pham LD, et al. Oxidative stress interferes with white matter renewal after prolonged cerebral hypoperfusion in mice. *Stroke* 2013; 44: 3516–3521.
19. Tsai TH, Sun CK, Su CH, et al. Sitagliptin attenuated brain damage and cognitive impairment in mice with chronic cerebral hypoperfusion through suppressing oxidative stress and inflammatory reaction. *J Hypertens* 2015; 33: 1001–1013.
20. Ueno Y, Koike M, Shimada Y, et al. L-carnitine enhances axonal plasticity and improves white-matter lesions after chronic hypoperfusion in rat brain. *J Cereb Blood Flow Metab* 2015; 35: 382–91.
21. Block ML, Zecca L and Hong JS. Microglia-mediated neurotoxicity: uncovering the molecular mechanisms. *Nat Rev Neurosci* 2007; 8: 57–69.
22. Cho KO, La HO, Cho YJ, et al. Minocycline attenuates white matter damage in a rat model of chronic cerebral hypoperfusion. *J Neurosci Res* 2006; 83: 285–291.
23. Liu Q, He S, Groysman L, et al. White matter injury due to experimental chronic cerebral hypoperfusion is associated with C5 deposition. *PLoS One* 2013; 8: e84802.
24. Lee KM, Bang J, Kim BY, et al. Fructus mume alleviates chronic cerebral hypoperfusion-induced white matter and hippocampal damage via inhibition of inflammation and downregulation of TLR4 and p38 MAPK signaling. *BMC Complement Altern Med* 2015; 15: 125.
25. Chen L, Yao Y, Wei C, et al. T cell immunity to glatiramer acetate ameliorates cognitive deficits induced by chronic cerebral hypoperfusion by modulating the microenvironment. *Sci Rep* 2015; 5: 14308.
26. Morsali D, Bechtold D, Lee W, et al. Safinamide and flecainide protect axons and reduce microglial activation in models of multiple sclerosis. *Brain* 2013; 136: 1067–1082.
27. Wang G, Shi Y, Jiang X, et al. HDAC inhibition prevents white matter injury by modulating microglia/macrophage polarization through the GSK3beta/PTEN/Akt axis. *Proc Natl Acad Sci USA* 2015; 112: 2853–2858.
28. Al-Jaderi Z and Maghazachi AA. Utilization of dimethyl fumarate and related molecules for treatment of multiple sclerosis, cancer, and other diseases. *Front Immunol* 2016; 7: 278.
29. Ellrichmann G, Petrasch-Parwez E, Lee DH, et al. Efficacy of fumaric acid esters in the R6/2 and YAC128 models of Huntington's disease. *PLoS One* 2011; 6: e16172.
30. Ahuja M, Ammal Kaidery N, Yang L, et al. Distinct Nrf2 signaling mechanisms of fumaric acid esters and their role in neuroprotection against 1-Methyl-4-Phenyl-1,2,3,6-tetrahydropyridine-induced experimental Parkinson's-like disease. *J Neurosci* 2016; 36: 6332–6351.
31. Jing X, Shi H, Zhang C, et al. Dimethyl fumarate attenuates 6-OHDA-induced neurotoxicity in SH-SY5Y cells and in animal model of Parkinson's disease by enhancing Nrf2 activity. *Neuroscience* 2015; 286: 131–140.
32. Lastres-Becker I, Garcia-Yague AJ, Scannevin RH, et al. Repurposing the NRF2 activator dimethyl fumarate as therapy against synucleinopathy in Parkinson's disease. *Antioxid Redox Signal* 2016; 25: 61–77.
33. Zhao X, Sun G, Zhang J, et al. Dimethyl fumarate protects brain from damage produced by intracerebral hemorrhage by mechanism involving Nrf2. *Stroke* 2015; 46: 1923–1928.
34. Liu Y, Qiu J, Wang Z, et al. Dimethyl fumarate alleviates early brain injury and secondary cognitive deficits after experimental subarachnoid hemorrhage via activation of Keap1-Nrf2-ARE system. *J Neurosurg* 2015; 123: 915–923.
35. Iniaghe LO, Krafft PR, Klebe DW, et al. Dimethyl fumarate confers neuroprotection by casein kinase 2 phosphorylation of Nrf2 in murine intracerebral hemorrhage. *Neurobiol Dis* 2015; 82: 349–358.



36. Yao Y, Miao W, Liu Z, et al. Dimethyl fumarate and monomethyl fumarate promote post-ischemic recovery in mice. *Trans Stroke Res* 2016; 7: 535–547.
37. Miljkovic D, Blazevski J, Petkovic F, et al. A comparative analysis of multiple sclerosis-relevant anti-inflammatory properties of ethyl pyruvate and dimethyl fumarate. *J Immunol* 2015; 194: 2493–2503.
38. Michell-Robinson MA, Moore CS, Healy LM, et al. Effects of fumarates on circulating and CNS myeloid cells in multiple sclerosis. *Ann Clin Trans Neurol* 2016; 3: 27–41.
39. Parodi B, Rossi S, Morando S, et al. Fumarates modulate microglia activation through a novel HCAR2 signaling pathway and rescue synaptic dysregulation in inflamed CNS. *Acta Neuropathol* 2015; 130: 279–295.
40. Schilling S, Goelz S, Linker R, et al. Fumaric acid esters are effective in chronic experimental autoimmune encephalomyelitis and suppress macrophage infiltration. *Clin Exp Immunol* 2006; 145: 101–107.
41. Linker RA, Lee DH, Ryan S, et al. Fumaric acid esters exert neuroprotective effects in neuroinflammation via activation of the Nrf2 antioxidant pathway. *Brain* 2011; 134: 678–692.
42. Schulze-Topphoff U, Varrin-Doyer M, Pekarek K, et al. Dimethyl fumarate treatment induces adaptive and innate immune modulation independent of Nrf2. *Proc Natl Acad Sci USA* 2016; 113: 4777–4782.
43. Crawford DK, Mangiardi M and Tiwari-Woodruff SK. Assaying the functional effects of demyelination and remyelination: revisiting field potential recordings. *J Neurosci Meth* 2009; 182: 25–33.
44. Crawford DK, Mangiardi M, Xia X, et al. Functional recovery of callosal axons following demyelination: a critical window. *Neuroscience* 2009; 164: 1407–1421.
45. Yamazaki Y, Hozumi Y, Kaneko K, et al. Oligodendrocytes: facilitating axonal conduction by more than myelination. *Neuroscientist* 2010; 16: 11–18.
46. Baltan S, Besancon EF, Mbow B, et al. White matter vulnerability to ischemic injury increases with age because of enhanced excitotoxicity. *J Neurosci* 2008; 28: 1479–1489.
47. Goncharenko K, Eftekharpour E, Velumian AA, et al. Changes in gap junction expression and function following ischemic injury of spinal cord white matter. *J Neurophysiol* 2014; 112: 2067–2075.
48. Hamner MA, Ye Z, Lee RV, et al. Ischemic preconditioning in white matter: magnitude and mechanism. *J Neurosci* 2015; 35: 15599–15611.
49. Reeves TM, Phillips LL and Povlishock JT. Myelinated and unmyelinated axons of the corpus callosum differ in vulnerability and functional recovery following traumatic brain injury. *Exp Neurol* 2005; 196: 126–137.
50. Zhang J, Liu J, Fox HS, et al. N-methyl-D-aspartate receptor-mediated axonal injury in adult rat corpus callosum. *J Neurosci Res* 2013; 91: 240–248.
51. Moore S, Patel R, Hannsun G, et al. Sex chromosome complement influences functional callosal myelination. *Neuroscience* 2013; 245: 166–178.
52. Patel R, Moore S, Crawford DK, et al. Attenuation of corpus callosum axon myelination and remyelination in the absence of circulating sex hormones. *Brain Pathol* 2013; 23: 462–475.
53. Corcoba A, Steullet P, Duarte JM, et al. Glutathione deficit affects the integrity and function of the fimbria/fornix and anterior commissure in mice: relevance for schizophrenia. *Int J Neuropsychopharmacol* 2015; 19: pyv110.
54. Park E, Eisen R, Kinio A, et al. Electrophysiological white matter dysfunction and association with neurobehavioral deficits following low-level primary blast trauma. *Neurobiol Dis* 2013; 52: 150–159.
55. Ritter J, Schmitz T, Chew LJ, et al. Neonatal hyperoxia exposure disrupts axon-oligodendrocyte integrity in the subcortical white matter. *J Neurosci* 2013; 33: 8990–9002.
56. Pryor J and Shi R. Electrophysiological changes in isolated spinal cord white matter in response to oxygen deprivation. *Spinal Cord* 2006; 44: 653–661.
57. Nashmi R and Fehlings MG. Changes in axonal physiology and morphology after chronic compressive injury of the rat thoracic spinal cord. *Neuroscience* 2001; 104: 235–251.
58. Reeves TM, Trimmer PA, Colley BS, et al. Targeting Kv1.3 channels to reduce white matter pathology after traumatic brain injury. *Exp Neurol* 2016; 283: 188–203.
59. Ito D, Tanaka K, Suzuki S, et al. Enhanced expression of Iba1, ionized calcium-binding adapter molecule 1, after transient focal cerebral ischemia in rat brain. *Stroke* 2001; 32: 1208–1215.
60. Fumagalli S, Perego C, Pischiutta F, et al. The ischemic environment drives microglia and macrophage function. *Front Neurol* 2015; 6: 81.
61. Moore S, Khalaj AJ, Patel R, et al. Restoration of axon conduction and motor deficits by therapeutic treatment with glatiramer acetate. *J Neurosci Res* 2014; 92: 1621–1636.
62. Neumann H. Molecular mechanisms of axonal damage in inflammatory central nervous system diseases. *Curr Opin Neurol* 2003; 16: 267–273.
63. Redford EJ, Kapoor R and Smith KJ. Nitric oxide donors reversibly block axonal conduction: demyelinated axons are especially susceptible. *Brain* 1997; 120(Pt 12): 2149–2157.
64. Lin R, Cai J, Kostuk EW, et al. Fumarate modulates the immune/inflammatory response and rescues nerve cells and neurological function after stroke in rats. *J Neuroinflamm* 2016; 13: 269.
65. Han R, Xiao J, Zhai H, et al. Dimethyl fumarate attenuates experimental autoimmune neuritis through the nuclear factor erythroid-derived 2-related factor 2/hemoxygenase-1 pathway by altering the balance of M1/M2 macrophages. *J Neuroinflamm* 2016; 13: 97.
66. Cho H, Hartsock MJ, Xu Z, et al. Monomethyl fumarate promotes Nrf2-dependent neuroprotection in retinal ischemia-reperfusion. *J Neuroinflamm* 2015; 12: 239.
67. Tanaka K, Nogawa S, Suzuki S, et al. Upregulation of oligodendrocyte progenitor cells associated with restoration of mature oligodendrocytes and myelination in peri-infarct area in the rat brain. *Brain Res* 2003; 989: 172–179.

68. Sun J, Fang Y, Chen T, et al. WIN55, 212-2 promotes differentiation of oligodendrocyte precursor cells and improve remyelination through regulation of the phosphorylation level of the ERK 1/2 via cannabinoid receptor 1 after stroke-induced demyelination. *Brain Res* 2013; 1491: 225–235.
69. Tanaka K, Nogawa S, Ito D, et al. Activation of NG2-positive oligodendrocyte progenitor cells during post-ischemic reperfusion in the rat brain. *Neuroreport* 2001; 12: 2169–2174.
70. Moharreh-Khiabani D, Blank A, Skripuletz T, et al. Effects of fumaric acids on cuprizone induced central nervous system de- and remyelination in the mouse. *PLoS One* 2010; 5: e11769.
71. Brennan MS, Patel H, Allaire N, et al. Pharmacodynamics of dimethyl fumarate are tissue specific and involve NRF2-dependent and -independent mechanisms. *Antioxid Redox Signal* 2016; 24: 1058–1071.
72. Reeves TM, Phillips LL, Lee NN, et al. Preferential neuroprotective effect of tacrolimus (FK506) on unmyelinated axons following traumatic brain injury. *Brain Res* 2007; 1154: 225–236.
73. Pitarokoli K, Ambrosius B, Meyer D, et al. Dimethyl fumarate ameliorates Lewis rat experimental autoimmune neuritis and mediates axonal protection. *PLoS One* 2015; 10: e0143416.
74. Ueno M, Tomimoto H, Akiguchi I, et al. Blood-brain barrier disruption in white matter lesions in a rat model of chronic cerebral hypoperfusion. *J Cereb Blood Flow Metab* 2002; 22: 97–104.
75. Kunze R, Urrutia A, Hoffmann A, et al. Dimethyl fumarate attenuates cerebral edema formation by protecting the blood-brain barrier integrity. *Exp Neurol* 2015; 266: 99–111.
76. Wilms H, Sievers J, Rickert U, et al. Dimethylfumarate inhibits microglial and astrocytic inflammation by suppressing the synthesis of nitric oxide, IL-1beta, TNF-alpha and IL-6 in an in-vitro model of brain inflammation. *J Neuroinflamm* 2010; 7: 30.
77. Yamagami S, Tamura M, Hayashi M, et al. Differential production of MCP-1 and cytokine-induced neutrophil chemoattractant in the ischemic brain after transient focal ischemia in rats. *J Leukocyte Biol* 1999; 65: 744–749.
78. Kim JS, Gautam SC, Chopp M, et al. Expression of monocyte chemoattractant protein-1 and macrophage inflammatory protein-1 after focal cerebral ischemia in the rat. *J Neuroimmunol* 1995; 56: 127–134.
79. Washida K, Ihara M, Nishio K, et al. Nonhypotensive dose of telmisartan attenuates cognitive impairment partially due to peroxisome proliferator-activated receptor-gamma activation in mice with chronic cerebral hypoperfusion. *Stroke* 2010; 41: 1798–1806.
80. Mirabelli-Badenier M, Braunersreuther V, Viviani GL, et al. CC and CXC chemokines are pivotal mediators of cerebral injury in ischaemic stroke. *Thromb Haemost* 2011; 105: 409–420.
81. Takami S, Nishikawa H, Minami M, et al. Induction of macrophage inflammatory protein MIP-1alpha mRNA on glial cells after focal cerebral ischemia in the rat. *Neurosci Lett* 1997; 227: 173–176.
82. Zechariah A, ElAli A, Doeppner TR, et al. Vascular endothelial growth factor promotes pericyte coverage of brain capillaries, improves cerebral blood flow during subsequent focal cerebral ischemia, and preserves the metabolic penumbra. *Stroke* 2013; 44: 1690–1697.
83. Wang J, Fu X, Yu L, et al. Preconditioning with VEGF enhances angiogenic and neuroprotective effects of bone marrow mononuclear cell transplantation in a rat model of chronic cerebral hypoperfusion. *Mol Neurobiol* 2016; 53: 6057–6068.
84. Wiesner D, Merdian I, Lewerenz J, et al. Fumaric acid esters stimulate astrocytic VEGF expression through HIF-1alpha and Nrf2. *PLoS One* 2013; 8: e76670.
85. Scheller J, Chalaris A, Schmidt-Arras D, et al. The pro- and anti-inflammatory properties of the cytokine interleukin-6. *Biochim Biophys Acta* 2011; 1813: 878–888.
86. Loddick SA, Turnbull AV and Rothwell NJ. Cerebral interleukin-6 is neuroprotective during permanent focal cerebral ischemia in the rat. *J Cereb Blood Flow Metab* 1998; 18: 176–179.
87. Murray KN, Parry-Jones AR and Allan SM. Interleukin-1 and acute brain injury. *Front Cell Neurosci* 2015; 9: 18.
88. Yoshizaki K, Adachi K, Kataoka S, et al. Chronic cerebral hypoperfusion induced by right unilateral common carotid artery occlusion causes delayed white matter lesions and cognitive impairment in adult mice. *Exp Neurol* 2008; 210: 585–591.
89. Lambertsen KL, Gregersen R, Meldgaard M, et al. A role for interferon-gamma in focal cerebral ischemia in mice. *J Neuropathol Exp Neurol* 2004; 63: 942–955.